Lymphatic PD-L1 Expression Restricts Tumor-Specific CD8$^+$ T-cell Responses

Nikola Cousin, Stefan Cap, Manuel Dihr, Carlotta Tacconi, Michael Detmar, and Lothar C. Dieterich

ABSTRACT

Lymph node (LN)–resident lymphatic endothelial cells (LEC) mediate peripheral tolerance by self-antigen presentation on MHC-I and constitutive expression of T-cell inhibitory molecules, including PD-L1 (CD274). Tumor-associated LECs also upregulate PD-L1, but the specific role of lymphatic PD-L1 in tumor immunity is not well understood. In this study, we generated a mouse model lacking lymphatic PD-L1 expression and challenged these mice with two orthotopic tumor models, B16F10 melanoma and MC38 colorectal carcinoma. Lymphatic PD-L1 deficiency resulted in consistent expansion of tumor-specific CD8$^+$ T cells in tumor-draining LNs in both tumor models, reduced primary tumor growth in the MC38 model, and increased efficacy of adoptive T-cell therapy in the B16F10 model. Strikingly, lymphatic PD-L1 acted primarily by inducing apoptosis in tumor-specific CD8$^+$ central memory T cells. Overall, these findings demonstrate that LECs restrain tumor-specific immunity via PD-L1, which may explain why some patients with cancer without PD-L1 expression in the tumor microenvironment still respond to PD-L1/PD-1–targeted immunotherapy.

Significance: A new lymphatic-specific PD-L1 knockout mouse model reveals that lymphatic endothelial PD-L1 expression reduces tumor immunity, inducing apoptosis in tumor-specific CD8$^+$ central memory cells in tumor-draining lymph nodes.

Introduction

Lymphatic vessels play an essential role in the generation of adaptive immune responses, transporting antigen and antigen-presenting cells (APC) from peripheral tissues to lymph nodes (LN), and freshly primed lymphocytes from the LNs to the central circulation. Within the LNs, lymphatic sinuses orchestrate the lymph flow, antigen entry into the parenchyma, and immune cell migration. Lymphatic endothelial cells (LEC) that line all lymphatic vessels and sinuses have recently emerged as direct, antigen-dependent and independent regulators of adaptive immunity, in particular of dendritic cells (DC) and T cells (1, 2). LN-residing LECs for instance express and present peripheral tissue self-antigens on MHC-I (3, 4), and thereby inhibit autoreactive T cells specific for those antigens (5, 6). They are also able to sample free antigen from the lymph and cross-present it on MHC-I under steady-state conditions (7). Thus, LN LECs have been suggested as important contributors to the maintenance of peripheral self-tolerance. On the other hand, LN LECs may also stimulate memory differentiation in a subset of T cells (8) and provide a long-term archive for antigen during virus infections (9), promoting T-cell immunity. In the tumor context, the role of LECs in regulating T-cell responses is not as clear. In the B16F10 melanoma model, tumor-associated and draining LN LECs have been found to present tumor antigen on MHC-I (10), whereas forced induction of LEC expansion via overexpression of the lymphangiogenic growth factor VEGF-C in tumor cells had inconsistent effects on tumor immunity and the efficacy of experimental immunotherapeutic approaches, depending on the time point (10, 11).

Another open question relates to the mechanism of LEC-mediated T-cell inhibition (or activation). Under steady-state conditions, LN LECs do not express co-stimulatory molecules, but instead express high levels of T-cell inhibitory molecules, including PD-L1 (CD274) (6). Systemic inhibition of the PD-L1/PD-1 axis facilitated autoimmune CD8$^+$ responses against the LEC-expressed self-antigen tyrosinase, demonstrating that PD-L1 is involved in peripheral tolerance (6). However, the precise function of PD-L1 expressed specifically by LECs has not been elucidated. Similarly, in tumor immunity, we and others have shown that tumor-associated LECs upregulate PD-L1 expression in mouse tumor models, probably in response to IFNγ produced in the tumor microenvironment (12, 13), and chimeric mice lacking PD-L1 expression in all radio-resistant stromal cells showed increased CD8$^+$ T-cell activation and a better response toward adoptive T-cell therapy (ACT) in the B16F10 model expressing ovalbumin (ova) as model antigen (B16-ova; ref. 13). However, multiple stromal cell types in the tumor microenvironment or the draining LNs may express PD-L1 and contribute to T-cell inhibition, so the precise function of LEC-expressed PD-L1 in tumor immunity has remained unknown. To clarify this question, we have generated a lymphatic-specific PD-L1^{ko} mouse model and have investigated CD8$^+$ T-cell responses in two independent syngeneic tumor models as well as in ACT.

Materials and Methods

Mice

PD-L1^{flox} mice (14) were obtained from Lexicon/Taconic and backcrossed to the C57BL/6 background by speed congenics before

Institute of Pharmaceutical Sciences, Swiss Federal Institute of Technology (ETH) Zurich, Zurich, Switzerland.

Note: Supplementary data for this article are available at Cancer Research Online (http://cancerres.aacrjournals.org/).

N. Cousin, S. Cap, and M. Dihr contributed equally as co-authors of this article.

Corresponding Author: Lothar C. Dieterich, ETH Zurich, Institute of Pharmaceutical Sciences, Vladimir-Prelog-Weg 1–5/10, 8093 Zurich, Switzerland. Phone: 41-44-63-37392; Fax: 41-44-63-31344; E-mail: lothar.dieterich@pharma.ethz.ch

Cancer Res 2021;81:4133–44

doi: 10.1158/0008-5472.CAN-21-0633

crossing them with Prox1-Cre-ER^{T2} mice (15), kindly provided by Dr. Taija Mäkinen (Uppsala University, Sweden) to create PD-L1^{LECKO} mice. To induce Cre-mediated recombination, these mice were treated with 50 mg/kg tamoxifen (Sigma) in sunflower oil for 5 days by intraperitoneal injection. 3–4 days after the last injection, mice were inoculated with tumor cells as described below. Cre-negative, PD-L1$^{fl/fl}$ littermates served as controls and were equally treated with tamoxifen. Ly5.1$^+$ OT-1 mice were kindly provided by Dr. Roman Spörri (ETH Zurich, Switzerland). All mice were bred and housed in an SOPF facility at ETH Zurich. All experimental procedures were approved by the responsible ethics committee (Kantonales Veterinäramt Zürich, licenses 5/18 and 92/18).

Cell lines

Immortalized mouse LECs (16) were maintained on dishes coated with 10 μg/mL fibronectin (Millipore) and 10 μg/mL collagen type-1 (Advanced Biomatrix) in DMEM/F12 medium (Gibco) supplemented with 20% FBS (Gibco), 56 μg/mL heparin (Sigma), 10 μg/mL EC growth supplement (Bio-Rad) and 1 U/mL recombinant mouse IFNγ (Peprotech) at 33°C, 5% CO_2. Before experiments, IFNγ was removed, and cells were shifted to 37°C. To delete PD-L1 expression, the CrispR–Cas9n double nickase approach was used essentially as described before (17). In brief, a pair of sgRNAs were designed for a target sequence in exon 3 of the mouse *Cd274* (coding for PD-L1) gene using the online tool at http://crispr.mit.edu and were cloned into pSpCas9n(BB)-2A-GFP (RRID:Addgene_48140). LECs were transfected with the vectors using polyethylenimine as described previously (18). 24 hours later, successfully transfected GFP$^+$ cells were isolated using a FACS ARIA II instrument (BD Biosciences) and expanded in culture. Cells with successful PD-L1 deletion were isolated by two rounds of FACS sorting after O/N stimulation with 100 ng/mL IFNγ and staining with PD-L1-PE/Cy7 (clone 10F.9G2, BioLegend 124314, RRID:AB_10643573, 1:200). Cells retaining PD-L1 expression were isolated simultaneously and served as controls.

To generate MC38 cells expressing chicken ovalbumin (MC38-ova), we cloned the full-length ovalbumin-coding sequence (RRID: Addgene_64599; ref. 19) into a modified lentiviral vector in which the transgene is driven by a pgk-promoter and followed by an internal ribosomal entry site and an eGFP sequence (20). Lentiviral particles were generated in HEK293T cells (RRID:CVCL_0063, kindly provided by Dr. Laure-Anne Ligeon, University of Zurich, Switzerland) using a third-generation packaging system. 48 hours after transformation, single GFP$^+$ MC38 colorectal carcinoma cells (kindly provided by Dr. Tiziana Schioppa, Humanitas Clinical and Research Center, Milan, Italy) were sorted into 96-well plates and expanded in DMEM (Gibco) with 10% FBS at 37°C, 5% CO_2. A clone with high GFP expression but identical growth kinetics to the parental MC38 cells was selected for all further experiments.

B16F10 cells expressing ovalbumin (B16-ova) were kindly provided by Dr. Sònia Tugues (University of Zurich, Switzerland), and cultured in DMEM supplemented with 10% FBS and 1.5 mg/mL G418 (Roche).

All cell lines were routinely (ca. 4 times/year) checked for *Mycoplasma* contamination using a PCR kit (Genlantis), and have been authenticated by short tandem repeat profiling (Microsynth AG). After thawing, tumor cells were cultured on average for 3 passages before injection into mice.

OT-1 priming *in vitro*

Priming experiments were performed essentially as described before (12). 10,000 PD-L1$^-$ and PD-L1$^+$ LECs were seeded in coated 96-well plates and cultured O/N (in quintuplicates). The following day, cells were pulsed with 1 ng/mL SIINFEKL peptide (AnaSpec) for 30 minutes, washed twice with PBS, and subsequently cocultured O/N with 100,000 CD8$^+$ T cells freshly isolated from spleens of naive Ly5.1$^+$ OT-1 mice by positive MACS separation (Miltenyi) in T-cell medium [RPMI supplemented with 10% FBS, pyruvate, non-essential amino acids, 10 mmol/L HEPES (all from Gibco) and 50 μmol/L β-ME; Sigma]. Subsequently, cells were stained with Zombie-Aqua (BioLegend 423102, 1:500), CD8-FITC (clone 53–6.7, BioLegend 100706, RRID:AB_312745, 1:200), CD69-APC/Cy7 (clone H1.2F3, BioLegend 104526, RRID:AB_10679041, 1:200), PD1-APC (clone RMP1–30, BioLegend 109112, RRID:AB_10612938, 1:200), PD-L1-PE (clone MIH5, Thermo Fisher 12–5982–82, RRID:AB_466089, 1:200), Ki67-eFluor450 (clone SolA15, Thermo Fisher 48–5698–82, RRID:AB_11149124, 1:200) and IFNγ-PE/Cy7 (clone XMG1.2, BioLegend 505826, RRID:AB_2295770, 1:200) using an intracellular staining kit (Thermo Fisher) according to the manufacturer's instructions. To determine proliferation, CFSE-loaded OT-1 cells were cocultured with LECs as described above, but for 72 hours. All data were acquired using a Cytoflex S instrument (Beckman Coulter) and analyzed using FlowJo v10.5.3 (BD Biosciences, RRID:SCR_008520).

Tumor models

For orthotopic tumor growth, 200,000 MC38-ova cells in 20 μL PBS were injected into the rectal mucosa and tumors were allowed to grow for 21 days until sacrifice. Alternatively, 200,000 B16-ova cells in 20 μL PBS were injected intradermally into the shaved flank skin and tumor growth was monitored by caliper measurements until the study endpoint.

Adoptive T-cell transfer

OT-1 effector T cells were generated by *ex vivo* culture of total Ly5.1$^+$ OT-1 splenocytes in T-cell medium supplemented with 1 ng/mL SIINFEKL peptide and 100 U/mL recombinant mouse IL2 (ImmunoTools) for 72 hours. In some cases, freshly isolated OT-1 T cells were used without prior activation. 1×10^6 OT-1 T cells in 100 μL unsupplemented RPMI were transferred by tail vein injection on day 10 after tumor cell inoculation. For the transfer of tumor-experienced CD8$^+$ T cells, the cells were MACS-isolated from B16-ova–draining inguinal and axillary LNs by positive selection (Miltenyi) and subsequently transferred into C57Bl/6 wild-type mice. Subsequently, these mice were challenged by injection of 50 μg ovalbumin protein (Sigma) into the hind paw. PBS was injected in the contralateral hind paw as control. In some cases, mice were also challenged with B16-ova tumor implantation as described above.

Flow cytometry

LN stromal cells were isolated and enriched as described before (21). The non-stromal fractions obtained after pre-digestion were pooled with one third of the stromal-enriched fraction and used for LN T-cell analyses. Tumors were digested in 3.5 mg/mL collagenase type IV (Gibco) in DMEM with 2% FBS and 1.2 mmol/L $CaCl_2$ for 30 minutes at 37°C and passed through a cell strainer before erythrocyte lysis using PharmLyse buffer (BD Biosciences). Spleens were dissociated mechanically over a cell strainer and erythrocyte lysis was performed. Cell suspensions were resuspended in FACS buffer (PBS, 1% FBS, 1 mmol/L EDTA, 0.02% NaN3) and treated with anti-CD16/CD32 (clone 93, BioLegend 101302, RRID:AB_312801, 1:100) for 20 minutes on ice before staining.

To determine PD-L1 expression in LN stromal cells, the remaining stromal-enriched fractions were stained with CD31-FITC (clone

MEC13.3, BD Biosciences 553372, RRID:AB_394818, 1:300), podoplanin-PE (clone 8.1.1, Thermo Fisher 12–5381–82, RRID: AB_1907439, 1:400), CD45-PerCP (clone 30-F11, BD Biosciences 557235, RRID:AB_396609, 1:100), PD-L1-APC (clone 10F.9G2, BioLegend 124312, RRID:AB_10612741, 1:200) or PD-L1-PE/Cy7 (clone 10F.9G2, BioLegend 124314, 1:200), and Zombie-NIR (BioLegend 423106, 1:500) or Zombie-Aqua and were analyzed on a FACS ARIA II or a FACS Fortessa instrument (both BD Biosciences). PD-L1 expression in primary tumor-associated LECs was determined using CD45-PE/Cy7 (clone 30-F11, BioLegend 103114, RRID:AB_312979, 1:200), CD31-PerCp/Cy5.5 (clone MEC13.3, BioLegend 102522, RRID: AB_2566761, 1:300), podoplanin-PE, PD-L1-APC, and Zombie-NIR. T-cell and myeloid responses were examined using Zombie-Aqua, Apotracker-Green (BioLegend 427401, 1:200), AnnexinV-APC (BioLegend 640932), CD45-PacificBlue (clone 30-F11, BioLegend 103126, RRID:AB_493535, 1:400), CD45.1 PerCp (BioLegend 110726, RRID: AB_893345, 1:100), CD3-PE/Cy7 (clone 145–2C11, BioLegend 100320, RRID:AB_312685, 1:400), CD8-FITC (1:400) or CD8-APC/Cy7 (clone 53–6.7, BioLegend 100714, RRID:AB_312753, 1:400) or CD8-BV650 (clone 53–6.7, BioLegend 100741, RRID:AB_11124344, 1:400), CD4-PerCp (clone GK1.5, BioLegend 100432, RRID: AB_893323, 1:100), CD25-BV605 (clone PC61, BioLegend 102035, RRID:AB_11126977, 1:400), CD69-APC/Cy7 (1:400), PD1-APC (1:200), CD44-BV650 (clone IM7, BioLegend 103049, RRID: AB_2562600, 1:800) or CD44-APC (clone IM7, BD Biosciences 559250, RRID:AB:_398661, 1:800), CD62L-Alexa700 (clone MEL-14, BioLegend 104426, RRID:AB_493719, 1:400), CX3CR1-BV605 (clone SA011F11, BioLegend 149027, RRID:AB_2565937, 1:200), CD11c-PE/Cy7 (clone N418, BioLegend 117318, RRID:AB_493568, 1:400), CD11b-BV605 (clone M1/70, BioLegend 101257, RRID: AB_2565431, 1:200), Ly-6G-FITC (clone 1A8, BD Biosciences 551460, RRID_394207, 1:400), F4/80-biotin (clone CI:A3–1, Bio-Rad MCA497BB, RRID:AB_323893, 1:200) followed by Streptavidin-PerCp (BioLegend 405213, 1:200), MHC-II-Alexa700 (clone M5/114.15.2, BioLegend 107622, RRID:AB_493727, 1:800), CD80-FITC (clone 16–10A1, Thermo Fisher 11–0801–85, RRID:AB_465134, 1:400), CD86-PE (clone GL1, Thermo Fisher 12–0862–85, RRID: AB_465770, 1:400) and PE-conjugated tetramers (control: H-2K^b-SIYRYYGL, ova: H-2K^b-SIINFEKL, pmel: H-2D^b-EGSRNQDWL, all NIH tetramer core facility, 1:800; p15e: H-2K^b-KSPWFTTL, MBL, 1:20), followed by intracellular staining with Foxp3-PE/eFluor610 (clone FJK-16s, Thermo Fisher 61–5773–82, RRID:AB_2574624, 1:200) or Ki67-eFluor450 and analysis on a 4 laser Cytoflex S instrument (Beckmann Coulter). Data were analyzed using FlowJo v10.5.3 (BD Biosciences).

Statistical analysis

Statistical analysis was done using GraphPad Prism (RRID: SCR_002798). Graphs show mean values ± standard deviation. Number of replicates and test details are indicated in the corresponding figure legends.

Results

Lymphatic PD-L1 impairs T-cell priming by LECs *in vitro*

We previously reported that antibody-mediated blockade of PD-L1 promoted the priming of naive CD8$^+$ OT-1 cells by SIINFEKL-presenting cultured mouse LECs (12). However, as PD-L1 is also expressed by CD8$^+$ OT-1 cells themselves and is induced upon activation, we could not rule out that antibody-mediated inhibition of endogenously expressed PD-L1 in CD8$^+$ OT-1 cells could have contributed to this effect. To elucidate the function of LEC-expressed PD-L1 specifically, we generated PD-L1^{ko} LECs using the CrispR–Cas9n approach. Wild-type LECs expressed surface PD-L1 under baseline conditions and upregulated it in response to IFNγ, whereas PD-L1^{ko} LECs had completely lost PD-L1 expression (**Fig. 1A** and **B**). When loaded with the SIINFEKL peptide, PD-L1^{ko} LECs were able to prime naive OT-1 cells more efficiently than wild-type LECs, resulting in increased expression of CD69, IFNγ, and a higher proliferation rate (**Fig. 1C–E**). In addition, PD-L1 and PD-1 expression were increased in OT-1 cells primed by PD-L1^{ko} LECs compared with wild-type LECs, most likely as part of a negative feedback mechanism (**Fig. 1F** and **G**). Together, these data demonstrate that PD-L1 expression by antigen-presenting LECs impairs priming of naive CD8$^+$ T cells *in vitro*.

Generation of a conditional, lymphatic-specific PD-L1^{ko} mouse model

To study the function of lymphatic PD-L1 *in vivo*, we generated a conditional, lymphatic-specific PD-L1^{ko} mouse model ("PD-L1^{LECKO} mice") by crossing PD-L1^{flox} mice (14) with the Prox1-Cre-ER^{T2} line (Supplementary Fig. S1A; ref. 15). As expected, PD-L1 was robustly expressed in LN LECs in naive PD-L1^{LECKO} mice, and was efficiently deleted upon tamoxifen treatment (Supplementary Fig. S1B–S1D). In contrast, Prox1-negative LN blood vascular endothelial cells had a lower baseline expression of PD-L1, which was not affected by tamoxifen (Supplementary Fig. S1E–S1F). Thus, PD-L1^{LECKO} mice are a suitable model to elucidate the effect of lymphatic PD-L1 on immune responses *in vivo*.

Lymphatic PD-L1 deletion amplifies tumor-specific CD8$^+$ T-cell responses

To elucidate the role of LEC-expressed PD-L1 in tumor-specific CD8$^+$ T-cell responses, we implanted B16-ova melanoma cells orthotopically into the flank skin of tamoxifen-treated PD-L1^{LECKO} mice. Cre$^-$ littermates served as controls. Primary tumor growth was not affected by lymphatic PD-L1 deletion (**Fig. 2A**), in line with a previous report showing that growth of B16-ova tumors was not affected in bone marrow-chimeric mice lacking stromal PD-L1 expression (13). In contrast to this report, however, we did not observe an increase in the frequency of CD8$^+$ T cells, neither in the primary tumor, nor in draining LNs or the spleen (**Fig. 2B**), suggesting that PD-L1 expression by stromal cells other than LECs controls overall accumulation of CD8$^+$ T cells in tumors. Next, we used flow cytometry to analyze the T-cell response in greater detail (Supplementary Fig. S2). Importantly, using tetramers to detect CD8$^+$ T cells specific for the SIINFEKL peptide derived from ovalbumin and the EGSRNQDWL peptide derived from the endogenous melanoma antigen pmel (gp100), which is expressed by B16F10 cells (22), we found a significant increase in the frequency of these cells in the draining inguinal and axillary LNs (both ova- and pmel-specific T cells) and the spleen (only pmel-specific T cells), but not in primary tumors (**Fig. 2C–E**). No changes in the activation profile or the memory status of the overall CD8$^+$ T-cell population could be detected, whereas the frequency of CD4$^+$ FoxP3$^+$ T$_{reg}$ cells was slightly reduced in the spleens of Cre$^+$ PD-L1^{LECKO} mice (Supplementary Fig. S3A–S3C). These data indicate that lymphatic PD-L1 limits priming, expansion or survival of tumor-specific CD8$^+$ T cells *in vivo*, particularly in tumor-draining LNs where lymphatic PD-L1 expression is constitutively high.

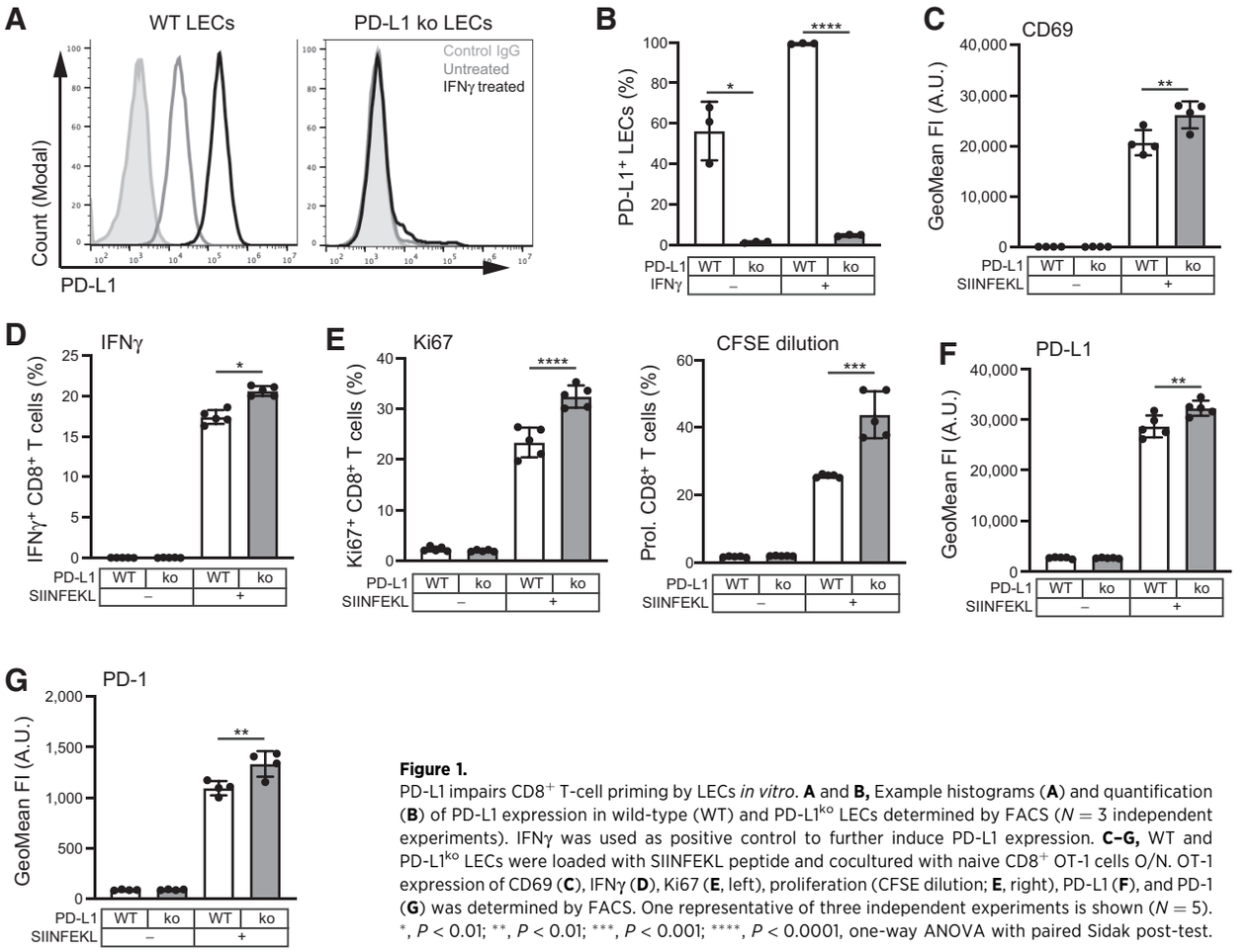

Figure 1.
PD-L1 impairs CD8$^+$ T-cell priming by LECs *in vitro*. **A** and **B,** Example histograms (**A**) and quantification (**B**) of PD-L1 expression in wild-type (WT) and PD-L1^{ko} LECs determined by FACS ($N = 3$ independent experiments). IFNγ was used as positive control to further induce PD-L1 expression. **C–G,** WT and PD-L1^{ko} LECs were loaded with SIINFEKL peptide and cocultured with naive CD8$^+$ OT-1 cells O/N. OT-1 expression of CD69 (**C**), IFNγ (**D**), Ki67 (**E**, left), proliferation (CFSE dilution; **E**, right), PD-L1 (**F**), and PD-1 (**G**) was determined by FACS. One representative of three independent experiments is shown ($N = 5$). *, $P < 0.01$; **, $P < 0.01$; ***, $P < 0.001$; ****, $P < 0.0001$, one-way ANOVA with paired Sidak post-test.

Because the B16F10 melanoma model is intrinsically resistant to systemic PD-1/PD-L1 blockade, we next sought to challenge PD-L1^{LECKO} mice with a second, sensitive tumor model. To this end, we engineered MC38 colorectal carcinoma cells to express ovalbumin and implanted them orthotopically into the rectal mucosa of PD-L1^{LECKO} mice and Cre$^-$ controls. Three weeks later, tumors, draining (caudal mesenteric and iliac) LNs, and spleens were collected and analyzed. Like in the B16F10 model (12, 13), tumor-associated lymphatic vessels strongly upregulated PD-L1 expression (**Fig. 2F**). Importantly, tumor weight at the endpoint was significantly reduced by lymphatic PD-L1 deletion in this model (**Fig. 2G**). Furthermore, although the total frequency of CD8$^+$ T cells was unchanged as in the B16-ova model (**Fig. 2H**), the frequency of ova-specific CD8$^+$ T cells was again increased in tumor-draining LNs, but not in primary tumors or the spleen, and the frequency of CD8$^+$ T cells specific for the endogenous tumor antigen p15e tended to be increased in tumor-draining LNs as well (**Fig. 2I–K**). Again, we found no major differences in the activation profile and the memory status of the total CD8$^+$ T-cell population in any of the organs analyzed (Supplementary Fig. S3D and S3E). Thus, lymphatic PD-L1 expression enhances primary tumor growth in the MC38 model and reduces the expansion of tumor-specific T cells independently of the tumor model and the site of tumor cell injection.

In addition to its role in T-cell regulation, lymphatic PD-L1 has also been suggested to have an LN LEC-intrinsic function, regulating LEC expansion and contraction in the course of inflammatory responses (23). However, in our hands, deletion of PD-L1 in LECs had no effect on the LEC frequency in tumor-draining LNs (Supplementary Fig. S4A and S4B).

Deletion of lymphatic PD-L1 increases the efficiency of adoptive T-cell therapy

Complete stromal PD-L1 deletion has previously been reported to augment the antitumor effect of ACT with pre-activated OT-1 cells in the B16-ova model (13). To test whether this effect was due to lymphatic PD-L1, we treated B16-ova–bearing PD-L1^{LECKO} mice with an intravenous transfer of pre-activated effector OT-1 cells on day 10 after tumor inoculation (**Fig. 3A**). The tumor weight at the endpoint (day 17) was clearly reduced in PD-L1^{LECKO} mice compared with Cre$^-$ controls (**Fig. 3B**), demonstrating that deletion of lymphatic PD-L1 augments the efficiency of ACT. We also performed ACT in MC38-ova–bearing mice, but in this case, tumors were completely eradicated irrespective of lymphatic

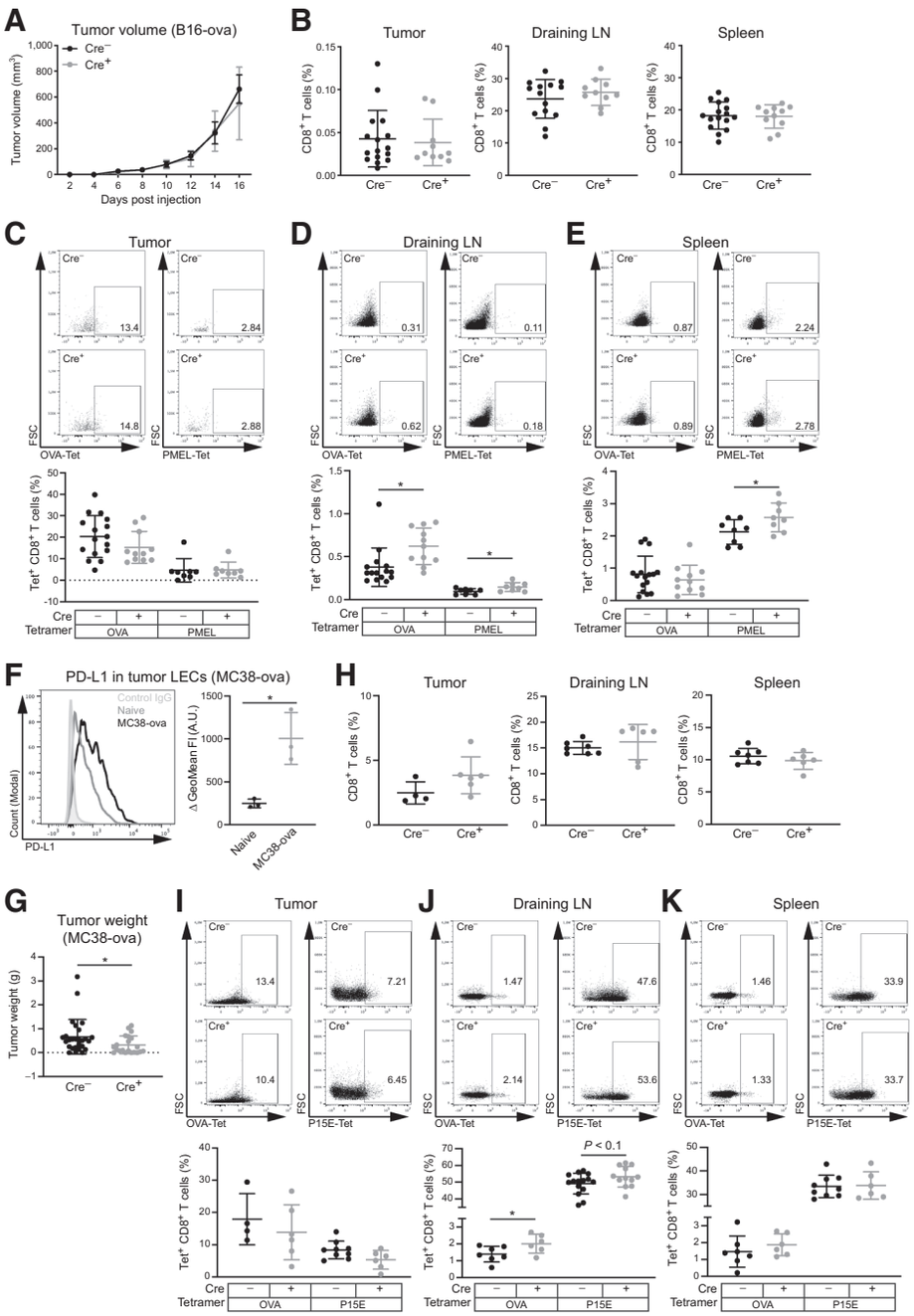

Figure 2.

Lymphatic PD-L1 reduces tumor-specific CD8$^+$ T-cell responses in mice bearing orthotopically implanted B16-ova melanomas and MC38-ova colorectal carcinomas. **A,** Growth of B16-ova cells in Cre$^+$ PD-L1^{LECKO} and Cre$^-$ controls [one representative of three independent experiments is shown ($N = 4$ Cre$^-$/5 Cre$^+$ mice)]. **B,** Quantification of CD8$^+$ T cells (expressed as the percentage of all living singlets) in tumor, draining LNs, and spleen on day 16 after inoculation of B16-ova cells. Data were pooled from three independent experiments ($N = 15$ Cre$^-$/11 Cre$^+$ mice). **C–E,** Representative FACS plots (pregated for CD8$^+$ T cells) and quantification of CD8$^+$ T cells specific for ova (ovalbumin) or pmel in tumors (**C**), draining LNs (**D**), and spleen ($N = 15$ Cre$^-$/11 Cre$^+$ mice for ova; $N = 8$ for pmel; **E**). **F,** Representative histogram (left) and quantification (right) of PD-L1 expression on LECs in normal colorectal mucosa (naive) compared with LECs in orthotopic MC38-ova tumors in Cre$^-$ control mice on day 21 after tumor cell inoculation ($N = 3$ mice/group). Graph represents the fluorescence intensity of PD-L1 compared with the isotype control. **G,** Weight of orthotopic MC38-ova tumors in Cre$^+$ PD-L1^{LECKO} mice and Cre$^-$ controls on day 21 after inoculation ($N = 27$ Cre$^-$/21 Cre$^+$ mice). **H,** Quantification of CD8$^+$ T cells in tumor, draining LNs, and spleen on day 21 after inoculation of MC38-ova cells ($N = 4$ Cre$^-$/6 Cre$^+$ mice in tumor; $N = 7$ Cre$^-$/6 Cre$^+$ mice in draining LN and spleen). **I–K,** Representative FACS plots (pre-gated for CD8$^+$ T cells) and quantification of CD8$^+$ T cells specific for ova and p15e in tumors (**I**), draining LNs (**J**), and spleen ($N = 4$ Cre$^-$/6 Cre$^+$ mice in tumor and $N = 7$ Cre$^-$/6 Cre$^+$ mice in draining LN and spleen for ova; $N = 9$ Cre$^-$/6 Cre$^+$ mice in tumor and spleen and $N = 15$ Cre$^-$/12 Cre$^+$ mice in draining LNs for p15e; **K**). *, $P < 0.05$, Student t test (**D, E, F,** and **J**) or Welch t test (**G**).

PD-L1 expression, preventing us from drawing further conclusions. Flow cytometry revealed an increased infiltration of CD8$^+$ T cells into B16-ova tumors in ACT-treated PD-L1^{LECKO} mice (**Fig. 3C**). In addition, we again noted an increased frequency of endogenous (CD45.1$^-$) ova-specific CD8$^+$ T cells in these mice in tumor-draining LNs (**Fig. 3D–F**). On the other hand, no changes in the frequency of transferred OT-1 cells could be detected (**Fig. 3G**), and their activation and memory profile were also equal between the two groups (Supplementary Fig. S4C and S4D). Thus, these data indicate that lymphatic PD-L1 primarily affects endogenously generated CD8$^+$ T-cell responses, which in cooperation with transferred exogenous effector cells can reduce tumor growth.

Lymphatic PD-L1 does not affect DC activation nor myeloid infiltrates

APCs such as DCs have been shown to express PD-1 (24, 25), and may receive inhibitory signals from PD-L1$^+$ LECs as they migrate from the tumor microenvironment to draining LNs. Thus, lymphatic PD-L1 may affect T-cell activation indirectly via DC inhibition. To investigate this further, we analyzed the phenotype of migratory (CD11^{int} MHC-II^{hi}) and resident (CD11c^{hi} MHC-II^{int})

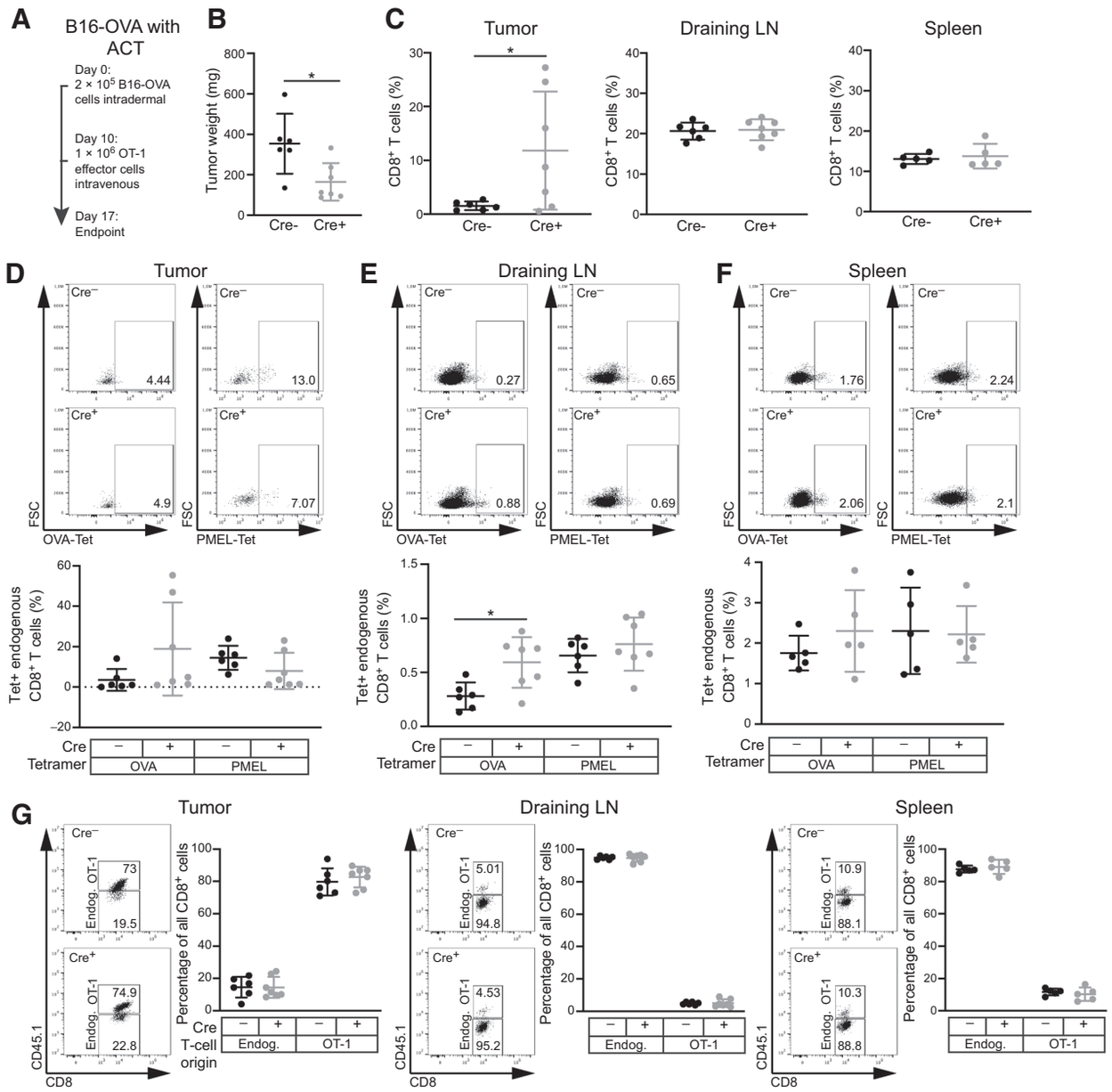

Figure 3.

Deletion of lymphatic PD-L1 increases the efficiency of adoptive T-cell transfer in the B16-ova melanoma model. **A,** Schematic representation of the adoptive T-cell therapy (ACT) approach in B16-ova–bearing mice. **B,** Primary tumor weight in Cre$^+$ PD-L1^{LECKO} mice and Cre$^-$ controls at the endpoint. **C,** Quantification of total CD8$^+$ T cells in tumor, draining LNs, and spleen. **D–F,** Representative FACS plots (pre-gated for endogenous, CD45.1$^-$ CD8$^+$ T cells) and quantification of endogenous CD8$^+$ T cells specific for ova (ovalbumin) or pmel in tumors (**D**), draining LNs (**E**), and spleen (**F**). **G,** Representative FACS plots (pre-gated for CD8$^+$ T cells) and quantification of CD45.1$^-$ endogenous and CD45.1$^+$-transferred OT-1 CD8$^+$ T cells in tumors, draining LNs, and spleens ($N = 6$ Cre$^-$/7 Cre$^+$ mice). *, $P < 0.05$, Student t test.

DCs in tumor-draining LNs, but found only low PD-1 expression and no changes in expression of the co-stimulatory molecules CD80 and CD86 after lymphatic PD-L1 deletion (Supplementary Fig. S5A–S5H). Furthermore, lymphatic PD-L1 deletion did not affect the frequency of LN macrophages [identified as CD11c$^{lo/int}$ MHC-II$^{lo/int}$ (ref. 26); Supplementary Fig. S5I and S5J] neither the infiltration of major myeloid immune cell types (granulocytes, DCs and monocytes/macrophages) nor their activation in the primary tumor tissue (Supplementary Fig. S5K–S5N).

Lymphatic PD-L1 regulates apoptosis in tumor-specific CD8$^+$ central memory cells

Previously, it has been suggested that LECs could trigger apoptosis of CD8$^+$ T cells *in vitro* (7). Thus, the increase in tumor-specific CD8$^+$ T cells in PD-L1^{LECKO} mice might be due to reduced apoptosis. Indeed,

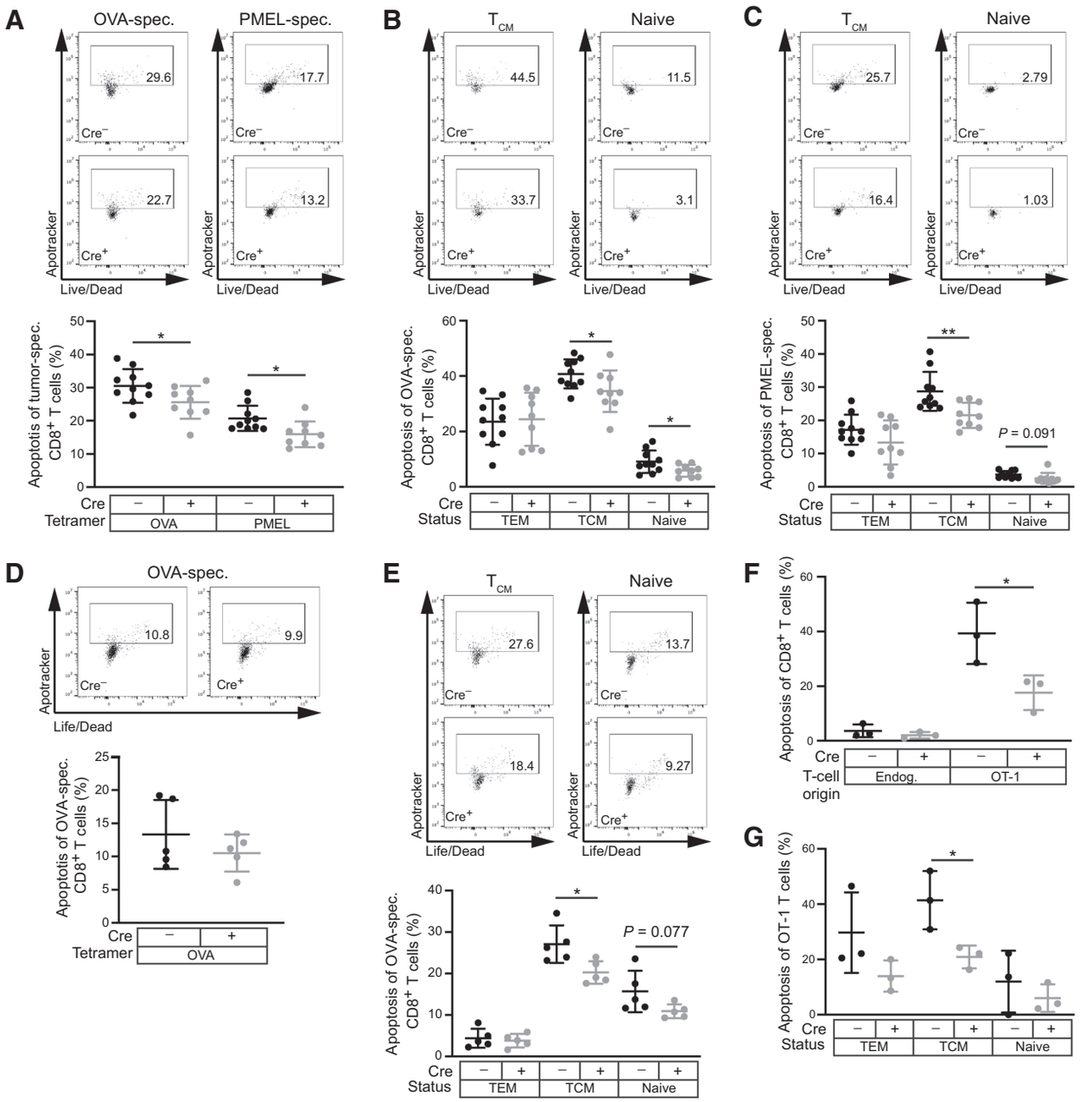

Figure 4.

Lymphatic PD-L1 induces apoptosis in tumor-specific CD8$^+$ central memory T cells in tumor-draining LNs. **A–C,** Representative FACS plots [pre-gated for tetramer-specific (**A**), ova-specific T_{CM} and naive (**B**) or pmel-specific T_{CM} and naive (**C**) CD8$^+$ T cells] and frequency of apoptotic cells [pooled early (Zombie$^-$) and late (Zombie$^+$) apoptotic] among all ova- and pmel-specific CD8$^+$ T cells (**A**) or within T_{EM}, T_{CM} and naive ova-specific (**B**) and pmel-specific (**C**) CD8$^+$ T cells in B16-ova–draining LNs ($N = 10$ Cre$^-$/9 Cre$^+$ mice). **D** and **E,** Representative FACS plots [pre-gated for all ova-specific (**D**) or ova-specific T_{CM} and naive (**E**) CD8$^+$ T cells] and frequency of apoptotic cells among all ova-specific CD8$^+$ T cells (**D**) or within T_{EM}, T_{CM} and naive ova-specific (**E**) CD8$^+$ T cells in MC38-ova–draining LNs ($N = 5$ mice/group). **F–G**, Apoptosis among endogenous and transferred CD45.1$^+$ OT-1 T cells (**F**) and among CD45.1$^+$ T_{EM}, T_{CM} and naive T cells (**G**) in B16-ova–draining LNs after adoptive transfer of freshly isolated, unstimulated OT-1 cells ($N = 3$ mice/group). *, $P < 0.05$; **, $P < 0.01$, Student t test.

we found that apoptosis of both ova- and pmel-specific CD8$^+$ T cells in B16-ova–draining LNs was significantly reduced after deletion of lymphatic PD-L1 (**Fig. 4A**), whereas the expression of Ki67 was not affected (Supplementary Fig. S6A). Surprisingly, further analysis of the apoptosis rate in tumor-specific CD44$^+$ CD62L$^-$ effector memory (T_{EM}), CD44$^+$ CD62L$^+$ central memory (T_{CM}) and CD44$^-$ CD62L$^-$ naive CD8$^+$ T cells revealed that lymphatic PD-L1 primarily affects apoptosis of T_{CM} cells (**Fig. 4B** and **C**). Essentially, the same results were obtained using AnnexinV-staining as a marker for apoptosis (Supplementary Fig. S6B and S6C). In contrast, tetramer-negative

$CD8^+$ T cells showed no difference in apoptosis between the groups (Supplementary Fig. S6D–S6F).

Among the T_{CM} cells, apoptosis was reduced specifically in the $CX3CR1^-$ subset of *bona fide* central memory cells (27), whereas $CX3CR1^{int}$ peripheral memory T cells showed no changes in apoptosis (Supplementary Fig. S6G). In line with this, we noted a selective expansion of ova-specific T_{CM} cells in B16-ova–draining LNs ($P < 0.08$; Supplementary Fig. S6H). Furthermore, proliferation and activation of ova-specific $CD8^+$ T_{EM}, T_{CM} and naive T cells were comparable between the groups (Supplementary Fig. S6I and S6J). Similar findings were made in the MC38-ova tumor model. Although the rate of apoptosis of all ova-specific $CD8^+$ T cells was not significantly altered in this case, ova-specific T_{CM} cells again showed reduced apoptosis in PD-$L1^{LECKO}$ mice compared with Cre^- controls (**Fig. 4D** and **E**).

ACT with pre-activated effector OT-1 cells did not lead to major differences in the transferred $CD45.1^+$ T cells in PD-$L1^{LECKO}$ compared with Cre^- controls (**Fig. 3G**; Supplementary Fig. S4C and S4D), perhaps because *ex vivo* activation had rendered these cells insensitive toward lymphatic PD-L1 expression. Accordingly, we found no differences in the rate of apoptosis of transferred effector OT-1 cells between the groups (Supplementary Fig. S6K). Therefore, we transferred freshly isolated, unstimulated OT-1 cells into B16-ova–bearing mice, and indeed found them to be less apoptotic in B16-ova–draining LNs of PD-$L1^{LECKO}$ recipients compared with Cre^- controls (**Fig. 4F**). This effect was LN-specific, as the rate of apoptosis of transferred naive OT-1 was equal between the groups in primary B16-ova tumors (Supplementary Fig. S6L). Further analysis revealed that apoptosis was most strongly reduced in OT-1 cells with a T_{CM} phenotype, which accounted for >50% of all OT-1 cells in tumor-draining LNs and tended to be more frequent in PD-$L1^{LECKO}$ mice (**Fig. 4G**; Supplementary Fig. S6M).

Tumor-specific $CD8^+$ memory T cells are more functional after lymphatic PD-L1 deletion

Finally, to test the functional relevance of reduced apoptosis in tumor-specific T_{CM} cells, we isolated $CD8^+$ T cells from B16-ova–draining LNs of PD-$L1^{LECKO}$ or Cre^- control mice and adoptively transferred them into C57BL/6 wild-type recipients. Then, we challenged these mice by injecting ovalbumin into the hind paw, selectively triggering activation of transferred ova-specific memory T cells, and analyzed the draining popliteal LN 24 hours later, using the contralateral, non-draining LN as control (**Fig. 5A**). Interestingly, the number of ova-specific $CD8^+$ T cells tended to be higher in mice that had received PD-$L1^{LECKO}$ T cells compared with recipients of Cre^- control T cells ($P = 0.052$, **Fig. 5B**). Furthermore, the ratio of ova-specific T_{EM} and T_{CM} cells in draining compared with non-draining LNs was significantly increased, as was the expression of CD69 and Ki67 (**Fig. 5C** and **D**). In line with this, recipients of $CD8^+$ T cells from B16-ova–bearing PD-$L1^{LECKO}$ mice also showed a modest survival benefit when challenged again with B16-ova tumors (**Fig. 5E** and **F**).

In conclusion, our data show that lymphatic PD-L1 limits tumor immunity predominantly by inducing apoptosis in tumor-specific $CD8^+$ T_{CM} cells in tumor-draining LNs, most likely via direct interactions between T cells and LECs (**Fig. 6**).

Discussion

Although PD-L1 is a well-known T-cell checkpoint molecule and immunotherapy targeting it or its receptor PD-1 has been impressively successful in a subset of patients suffering from several cancer types, the precise modalities and characteristics of its inhibitory effects on the immune system, for example, with regards to the various phases of a typical T-cell response such as priming, expansion, exhaustion, constriction and memory formation, are still not well understood (28). Furthermore, because PD-L1 may be expressed or induced in various cell types, including stromal cell populations, the most relevant sites and cell types for PD-L1 action during tumor immunity are still controversial. For example, contradictory results have been published regarding the role of PD-L1 expressed by tumor cells as compared with host cells in several tumor models, including the B16F10 and the MC38 model. Although some studies indicate that PD-L1 expression by tumor cells is sufficient to impair tumor immunity, most studies currently conclude that host PD-L1 is critically important (29–32). In line with this, it is becoming increasingly clear that PD-L1 expression by tumor cells alone is no reliable predictor of responsiveness to PD-1/PD-L1–targeting therapies (33), further suggesting that PD-L1 expression by host cells may be equally (or even more) relevant for tumor immunity and immunotherapy outcomes.

Recently, Lane and colleagues (13) demonstrated that PD-L1 in both hematopoietic and radio-resistant (stromal) cells affected T-cell responses in the B16F10 melanoma model. Yet, it remained unclear which stromal cell types were involved. Our data reveal that PD-L1 expressed by LECs contributes to tumor immune evasion via a distinctive mechanism primarily regulating apoptosis of tumor-specific $CD8^+$ T_{CM} cells. Deletion of lymphatic PD-L1 resulted in the expansion of tumor-specific $CD8^+$ T cells in tumor-draining LNs, where PD-L1 expression by LECs is constitutively high. Although this resulted in reduced growth of MC38 tumors that are sensitive to systemic PD-L1/PD-1 inhibition, it had no major effect on the growth of B16F10 tumors that are poorly immunogenic and inherently resistant to PD-L1/PD-1 blockade (34–37). One has to keep in mind that Prox1 is not completely specific for LECs, but is also expressed by some other cell types, including certain neurons and hepacytoes. However, it is very unlikely that PD-L1 deletion in these cell types may have affected T-cell responses in tumor-draining LNs. In contrast, complete stromal PD-L1 deletion had broader effects on the $CD8^+$ T-cell response in B16F10-bearing mice, including an overall increased accumulation of $CD8^+$ T cells in the primary tumor, most likely due to PD-L1 expression in stromal cells other than LECs (13). All in all, our data may explain why some patients with cancer without measurable PD-L1 expression in the tumor microenvironment still respond to PD-1/PD-L1–targeting therapies. Consequently, assessment of PD-L1 expression in tumor-associated and, maybe more importantly, draining LN residing LECs might be useful as an additional predictive biomarker to select patients for this kind of therapy.

PD-L1 expression is induced in primary tumor-associated LECs (12, 13), and could thus inhibit or delete PD-1^+ T_{EM} and T_{CM} cells that recirculate from the tumor microenvironment to tumor-draining LNs via the lymphatic system (38). In addition, PD-L1 expression is constitutively high in LN LECs (6), both in cells lining the floor of the subcapsular sinus and the medullary sinuses (5, 39). PD-L1 expressed by either of these LEC subsets could again affect recirculating T cells that enter the LN via afferent lymphatics (40, 41). In addition, medullary LEC-expressed PD-L1 might interact with PD-1^+ T cells exiting the LN via efferent lymphatics, such as T_{CM} cells that previously entered the LN via the blood circulation and freshly primed T cells, which are sensitive to PD-L1/PD-1 inhibition (42). Another subset of T cells important for tumor immunity is tissue-resident memory (T_{RM}) T cells. Recently, it was

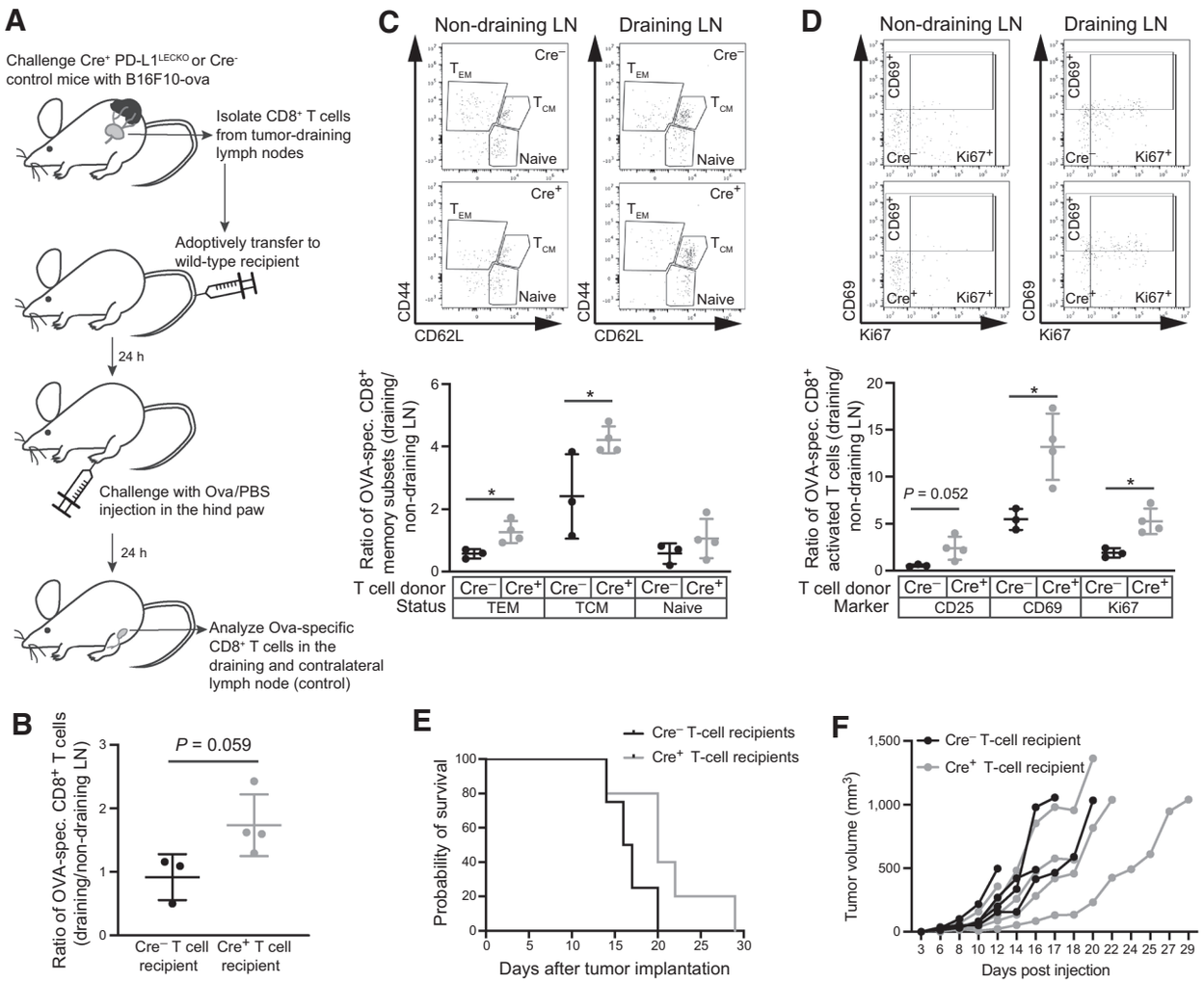

Figure 5.

Lymphatic PD-L1 deletion increases the functionality of tumor-specific memory T cells. **A,** C57Bl/6 wild-type mice received an adoptive transfer of $CD8^+$ T cells from B16-ova–draining LNs of PD-$L1^{LECKO}$ mice or Cre^- controls and were subsequently challenged by ovalbumin injection into the hind paw. **B,** Ratio of the absolute number of ova-specific $CD8^+$ T cells in challenged (draining) popliteal LNs compared with contralateral (non-draining) popliteal LNs. **C** and **D,** Representative FACS plots (pre-gated for ova-specific $CD8^+$ T cells) and ratio of ova-specific $CD8^+$ T_{EM}, T_{CM}, and naive (**F**) or activated (**G**) T cells in challenged (draining) versus contralateral (non-draining) popliteal LNs ($N = 3$ Cre^-/4 Cre^+ mice). **E** and **F,** C67Bl/6 wild-type mice received T cells as in **A** and were subsequently challenged with B16-ova tumor cells. Graphs show survival (**E**) and tumor volume (**F**) for each individual mouse ($N = 4$ Cre^-/5 Cre^+ mice). *, $P < 0.05$; Student t test.

shown that T_{RM} cells in peripheral tissues are rapidly stimulated by professional APCs but also by stromal cells (43). However, because tumor-associated LECs only represent a very small fraction of the stroma in the tumor microenvironment, we do not anticipate a strong influence of lymphatic PD-L1 deletion on T_{RM} cells within the tumor. Yet, T_{RM} cells are also present in LNs (44) where they could be affected by lymphatic PD-L1 expression. Our data do not allow us to determine precisely whether lymphatic PD-L1 affects T cells entering tumor-draining LNs via lymphatic or blood vessels. Nonetheless, they clearly demonstrate that lymphatic PD-L1 primarily acts on T cells with a classic T_{CM} phenotype ($CD44^+$ $CD62L^+$ $CX3CR1^-$), whereas T_{EM} and naive T cells were not or only marginally affected. This is somewhat surprising, given that T_{EM} cells are enriched among the T cells recirculating from the tumor microenvironment (38) and expressed the highest level of PD-1, followed by T_{CM} cells with intermediate PD-1 expression and naive T cells that were essentially $PD\text{-}1^-$ (Supplementary Fig. S6J). Possibly, tumor-derived T_{EM} cells are already dysfunctional due to their journey through the tumor microenvironment, and thus are not sensitive to additional inhibition by lymphatic PD-L1. In addition, there are reports that T_{EM} and T_{CM} cells differ in their expression of anti- and pro-apoptotic molecules, which could result in divergent sensitivity to PD-L1–induced apoptosis. For instance, *in vitro* generated $CD8^+$ T_{EM} cells expressed more Bcl-2 than T_{CM} cells and were less sensitive to apoptosis induction using a Bcl-2 inhibitor (45). On the other hand, virus-specific T_{CM} cells expressed more Bcl-2, but also more pro-apoptotic Bim in an LCMV infection

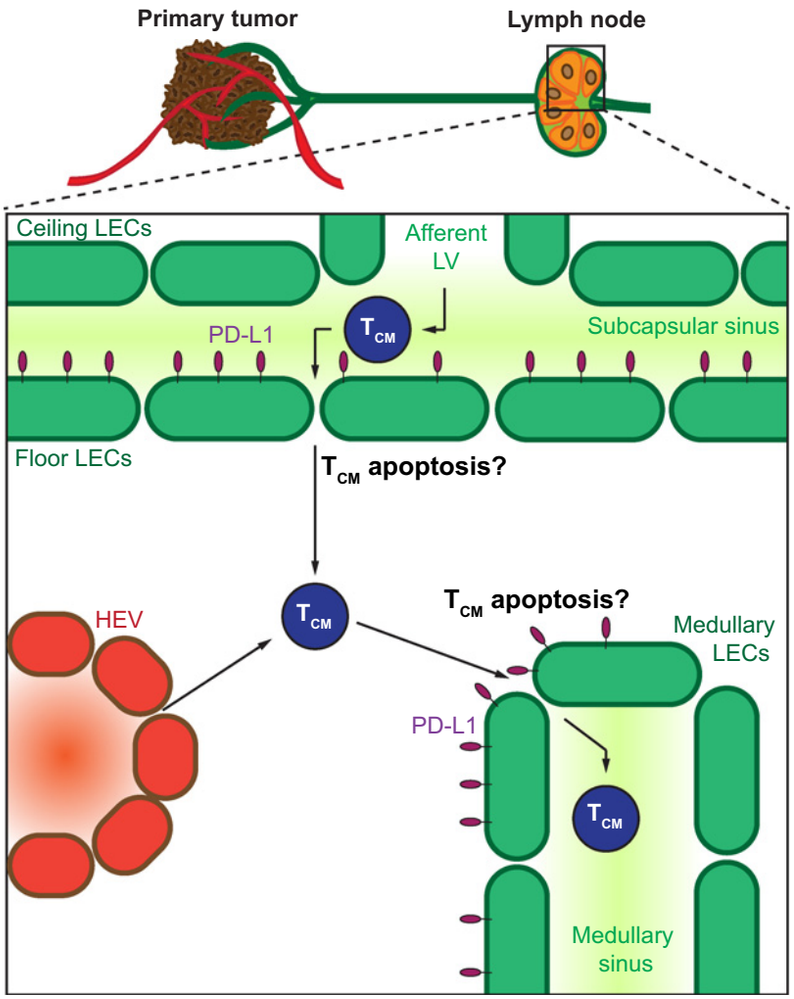

Figure 6.
Schematic representation of the proposed role of lymphatic PD-L1 in tumor immunity. Within LNs, LECs lining the floor of the subcapsular sinus as well as medullary sinuses express high levels of PD-L1. Tumor-specific T_{CM} cells may enter tumor-draining LNs either via high endothelial venules (HEV) or through afferent lymphatic vessels (LV), and will leave the LNs again via cortical and medullary lymphatic sinuses. Thus, T_{CM} cells may receive apoptosis-inducing signals from PD-L1$^+$ floor LECs as they enter the LN or from PD-L1$^+$ medullary LECs as they leave the LN.

model in mice (46). Further studies are needed to investigate the expression levels of these and other apoptosis-regulating molecules in T-cell subsets in a tumor context.

The primary effect of lymphatic PD-L1 deletion on tumor-specific T_{CM} cells was reduced apoptosis induction, whereas proliferation and activation of these cells were not significantly affected in tumor-bearing mice (Supplementary Fig. S6I and S6J). This was surprising given that PD-1 stimulation is generally believed to inhibit T-cell proliferation and effector functions (47, 48). However, PD-1 signaling also impairs the PI3K–Akt pathway involved in cell survival and has been shown to impair expression of the anti-apoptotic protein Bcl-x_L (49). Congruently, PD-L1 expression by tumor cells induced effector T-cell apoptosis *in vitro* and *in vivo* (50), and ova-presenting LECs upregulated PD-L1 when cultured together with naive OT-1 T cells and induced their apoptosis during priming (7). Together, these and our data suggest that LECs can induce apoptosis of both freshly primed and memory T cells via PD-L1.

In conclusion, our data reveal that LECs contribute to tumor immune evasion via PD-L1–mediated apoptosis induction in tumor-specific CD8$^+$ T_{CM} cells, and warrant further studies to investigate the predictive value of lymphatic PD-L1 expression for cancer immunotherapy.

Authors' Disclosures

L.C. Dieterich reports grants from Krebsliga Zurich and Vontobel Foundation during the conduct of the study. No disclosures were reported by the other authors.

Authors' Contributions

N. Cousin: Investigation, writing–review and editing. **S. Cap:** Formal analysis, investigation. **M. Dihr:** Formal analysis, investigation. **C. Tacconi:** Methodology, writing–review and editing. **M. Detmar:** Conceptualization, resources, supervision, funding acquisition, writing–review and editing. **L.C. Dieterich:** Conceptualization, resources, data curation, formal analysis, supervision, funding acquisition, investigation, writing–original draft, writing–review and editing.

Acknowledgments

The authors thank Jeannette Scholl (ETH Zurich) for technical support, and Dr. Roman Spörri (ETH Zurich) and the NIH tetramer core facility for provision of vital reagents. This work was supported by ERC grant LYVICAM and Swiss National Science Foundation grants 310030_166490 and 310030B_185392 (to M. Detmar), and a career seed grant by ETH Zurich and research grants from the Vontobel Foundation and Krebsliga Zurich (to L.C. Dieterich).

The costs of publication of this article were defrayed in part by the payment of page charges. This article must therefore be hereby marked *advertisement* in accordance with 18 U.S.C. Section 1734 solely to indicate this fact.

Received February 23, 2021; revised April 23, 2021; accepted June 1, 2021; published first June 7, 2021.

References

1. Ma Q, Dieterich LC, Detmar M. Multiple roles of lymphatic vessels in tumor progression. Curr Opin Immunol 2018;53:7–12.
2. Maisel K, Sasso MS, Potin L, Swartz MA. Exploiting lymphatic vessels for immunomodulation: rationale, opportunities, and challenges. Adv Drug Deliv Rev 2017;114:43–59.
3. Cohen JN, Guidi CJ, Tewalt EF, Qiao H, Rouhani SJ, Ruddell A, et al. Lymph node-resident lymphatic endothelial cells mediate peripheral tolerance via Aire-independent direct antigen presentation. J Exp Med 2010;207:681–8.
4. Fletcher AL, Lukacs-Kornek V, Reynoso ED, Pinner SE, Bellemare-Pelletier A, Curry MS, et al. Lymph node fibroblastic reticular cells directly present peripheral tissue antigen under steady-state and inflammatory conditions. J Exp Med 2010;207:689–97.
5. Cohen JN, Tewalt EF, Rouhani SJ, Buonomo EL, Bruce AN, Xu X, et al. Tolerogenic properties of lymphatic endothelial cells are controlled by the lymph node microenvironment. PLoS ONE 2014;9:e87740.
6. Tewalt EF, Cohen JN, Rouhani SJ, Guidi CJ, Qiao H, Fahl SP, et al. Lymphatic endothelial cells induce tolerance via PD-L1 and lack of costimulation leading to high-level PD-1 expression on CD8 T cells. Blood 2012;120:4772–82.
7. Hirosue S, Vokali E, Raghavan VR, Rincon-Restrepo M, Lund AW, Corthesy-Henrioud P, et al. Steady-state antigen scavenging, cross-presentation, and $CD8^+$ T-cell priming: a new role for lymphatic endothelial cells. J Immunol 2014;192:5002–11.
8. Vokali E, Yu SS, Hirosue S, Rincon-Restrepo M, V Duraes F, Scherer S, et al. Lymphatic endothelial cells prime naive CD8(+) T cells into memory cells under steady-state conditions. Nat Commun 2020;11:538.
9. Tamburini BA, Burchill MA, Kedl RM. Antigen capture and archiving by lymphatic endothelial cells following vaccination or viral infection. Nat Commun 2014;5:3989.
10. Lund AW, Duraes FV, Hirosue S, Raghavan VR, Nembrini C, Thomas SN, et al. VEGF-C promotes immune tolerance in B16 melanomas and cross-presentation of tumor antigen by lymph node lymphatics. Cell Rep 2012;1:191–9.
11. Fankhauser M, Broggi MAS, Potin L, Bordry N, Jeanbart L, Lund AW, et al. Tumor lymphangiogenesis promotes T-cell infiltration and potentiates immunotherapy in melanoma. Sci Transl Med 2017;9:eaal4712.
12. Dieterich LC, Ikenberg K, Cetintas T, Kapaklikaya K, Hutmacher C, Detmar M. Tumor-associated lymphatic vessels upregulate PDL1 to inhibit T-cell activation. Front Immunol 2017;8:66.
13. Lane RS, Femel J, Breazeale AP, Loo CP, Thibault G, Kaempf A, et al. IFNgamma-activated dermal lymphatic vessels inhibit cytotoxic T cells in melanoma and inflamed skin. J Exp Med 2018;215:3057–74.
14. Carter LL, Leach MW, Azoitei ML, Cui J, Pelker JW, Jussif J, et al. PD-1/PD-L1, but not PD-1/PD-L2, interactions regulate the severity of experimental autoimmune encephalomyelitis. J Neuroimmunol 2007;182:124–34.
15. Bazigou E, Lyons OT, Smith A, Venn GE, Cope C, Brown NA, et al. Genes regulating lymphangiogenesis control venous valve formation and maintenance in mice. J Clin Invest 2011;121:2984–92.
16. Vigl B, Aebischer D, Nitschke M, Iolyeva M, Rothlin T, Antsiferova O, et al. Tissue inflammation modulates gene expression of lymphatic endothelial cells and dendritic cell migration in a stimulus-dependent manner. Blood 2011;118:205–15.
17. Ran FA, Hsu PD, Wright J, Agarwala V, Scott DA, Zhang F. Genome engineering using the CRISPR-Cas9 system. Nat Protoc 2013;8:2281–308.
18. Hsu CY, Uludag H. A simple and rapid nonviral approach to efficiently transfect primary tissue-derived cells using polyethylenimine. Nat Protoc 2012;7:935–45.
19. Diebold SS, Cotten M, Koch N, Zenke M. MHC class II presentation of endogenously expressed antigens by transfected dendritic cells. Gene Ther 2001;8:487–93.
20. Dieterich LC, Huang H, Massena S, Golenhofen N, Phillipson M, Dimberg A. AlphaB-crystallin/HspB5 regulates endothelial-leukocyte interactions by enhancing NF-kappaB-induced upregulation of adhesion molecules ICAM-1, VCAM-1 and E-selectin. Angiogenesis 2013;16:975–83.
21. Commerford CD, Dieterich LC, He Y, Hell T, Montoya-Zegarra JA, Noerrelykke SF, et al. Mechanisms of tumor-induced lymphovascular niche formation in draining lymph nodes. Cell Rep 2018;25:3554–63 e4.
22. Tsukamoto K, Hirata S, Osada A, Kitamura R, Shimada S. Detection of circulating melanoma cells by RT-PCR amplification of three different melanocyte-specific mRNAs in a mouse model. Pigment Cell Res 2000;13:185–9.
23. Lucas ED, Finlon JM, Burchill MA, McCarthy MK, Morrison TE, Colpitts TM, et al. Type 1 IFN and PD-L1 coordinate lymphatic endothelial cell expansion and contraction during an inflammatory immune response. J Immunol 2018;201:1735–47.
24. Gordon SR, Maute RL, Dulken BW, Hutter G, George BM, McCracken MN, et al. PD-1 expression by tumour-associated macrophages inhibits phagocytosis and tumour immunity. Nature 2017;545:495–9.
25. Strauss L, Mahmoud MAA, Weaver JD, Tijaro-Ovalle NM, Christofides A, Wang Q, et al. Targeted deletion of PD-1 in myeloid cells induces antitumor immunity. Sci Immunol 2020;5:eaay1863.
26. Tacconi C, Commerford CD, Dieterich LC, Schwager S, He Y, Ikenberg K, et al. CD169(+) lymph node macrophages have protective functions in mouse breast cancer metastasis. Cell Rep 2021;35:108993.
27. Gerlach C, Moseman EA, Loughhead SM, Alvarez D, Zwijnenburg AJ, Waanders L, et al. The chemokine receptor CX3CR1 defines three antigen-experienced cd8 T-cell subsets with distinct roles in immune surveillance and homeostasis. Immunity 2016;45:1270–84.
28. Sharpe AH, Pauken KE. The diverse functions of the PD1 inhibitory pathway. Nat Rev Immunol 2018;18:153–67.
29. Juneja VR, McGuire KA, Manguso RT, LaFleur MW, Collins N, Haining WN, et al. PD-L1 on tumor cells is sufficient for immune evasion in immunogenic tumors and inhibits CD8 T-cell cytotoxicity. J Exp Med 2017;214:895–904.
30. Lau J, Cheung J, Navarro A, Lianoglou S, Haley B, Totpal K, et al. Tumour and host cell PD-L1 is required to mediate suppression of antitumour immunity in mice. Nat Commun 2017;8:14572.
31. Lin H, Wei S, Hurt EM, Green MD, Zhao L, Vatan L, et al. Host expression of PD-L1 determines efficacy of PD-L1 pathway blockade-mediated tumor regression. J Clin Invest 2018;128:805–15.
32. Tang H, Liang Y, Anders RA, Taube JM, Qiu X, Mulgaonkar A, et al. PD-L1 on host cells is essential for PD-L1 blockade-mediated tumor regression. J Clin Invest 2018;128:580–8.
33. Havel JJ, Chowell D, Chan TA. The evolving landscape of biomarkers for checkpoint inhibitor immunotherapy. Nat Rev Cancer 2019;19:133–50.
34. Huang L, Li Y, Du Y, Zhang Y, Wang X, Ding Y, et al. Mild photothermal therapy potentiates anti–PD-L1 treatment for immunologically cold tumors via an all-in-one and all-in-control strategy. Nat Commun 2019;10:4871.
35. Sanchez-Paulete AR, Cueto FJ, Martinez-Lopez M, Labiano S, Morales-Kastresana A, Rodriguez-Ruiz ME, et al. Cancer immunotherapy with immunomodulatory anti-CD137 and anti–PD-1 monoclonal antibodies requires BATF3-dependent dendritic cells. Cancer Discov 2016;6:71–9.
36. Yu JW, Bhattacharya S, Yanamandra N, Kilian D, Shi H, Yadavilli S, et al. Tumor-immune profiling of murine syngeneic tumor models as a framework to guide mechanistic studies and predict therapy response in distinct tumor microenvironments. PLoS ONE 2018;13:e0206223.
37. Zhou Z, Zhang B, Zai W, Kang L, Yuan A, Hu Y, et al. Perfluorocarbon nanoparticle-mediated platelet inhibition promotes intratumoral infiltration of T cells and boosts immunotherapy. Proc Natl Acad Sci U S A. 2019;116:11972–7.
38. Torcellan T, Hampton HR, Bailey J, Tomura M, Brink R, Chtanova T. *In vivo* photolabeling of tumor-infiltrating cells reveals highly regulated egress of T-cell subsets from tumors. Proc Natl Acad Sci U S A. 2017;114:5677–82.
39. Fujimoto N, He Y, D'Addio M, Tacconi C, Detmar M, Dieterich LC. Single-cell mapping reveals new markers and functions of lymphatic endothelial cells in lymph nodes. PLoS Biol 2020;18:e3000704.
40. Braun A, Worbs T, Moschovakis GL, Halle S, Hoffmann K, Bolter J, et al. Afferent lymph-derived T cells and DCs use different chemokine receptor CCR7-dependent routes for entry into the lymph node and intranodal migration. Nat Immunol 2011;12:879–87.
41. Martens R, Permanyer M, Werth K, Yu K, Braun A, Halle O, et al. Efficient homing of T cells via afferent lymphatics requires mechanical arrest and integrin-supported chemokine guidance. Nat Commun 2020;11:1114.
42. Ahn E, Araki K, Hashimoto M, Li W, Riley JL, Cheung J, et al. Role of PD-1 during effector CD8 T-cell differentiation. Proc Natl Acad Sci U S A 2018;115:4749–54.
43. Low JS, Farsakoglu Y, Amezcua Vesely MC, Sefik E, Kelly JB, Harman CCD, et al. Tissue-resident memory T-cell reactivation by diverse antigen-presenting cells imparts distinct functional responses. J Exp Med 2020;217:e20192291.
44. Beura LK, Wijeyesinghe S, Thompson EA, Macchietto MG, Rosato PC, Pierson MJ, et al. T cells in nonlymphoid tissues give rise to lymph-node-resident memory t cells. Immunity 2018;48:327–38.

45. Cippa PE, Gabriel SS, Kraus AK, Chen J, Wekerle T, Guimezanes A, et al. Bcl-2 inhibition to overcome memory cell barriers in transplantation. Am J Transplant 2014;14:333–42.
46. Kurtulus S, Tripathi P, Moreno-Fernandez ME, Sholl A, Katz JD, Grimes HL, et al. Bcl-2 allows effector and memory $CD8^+$ T cells to tolerate higher expression of Bim. J Immunol 2011;186:5729–37.
47. He X, Xu C. Immune checkpoint signaling and cancer immunotherapy. Cell Res 2020;30:660–669.
48. Boussiotis VA. Molecular and biochemical aspects of the PD-1 checkpoint pathway. N Engl J Med 2016;375:1767–78.
49. Parry RV, Chemnitz JM, Frauwirth KA, Lanfranco AR, Braunstein I, Kobayashi SV, et al. CTLA-4 and PD-1 receptors inhibit T-cell activation by distinct mechanisms. Mol Cell Biol 2005;25:9543–53.
50. Dong H, Strome SE, Salomao DR, Tamura H, Hirano F, Flies DB, et al. Tumor-associated B7-H1 promotes T-cell apoptosis: a potential mechanism of immune evasion. Nat Med 2002;8:793–800.